Korean J. Chem. Eng., 34(4), 1187-1191 (2017)
DOI: 10.1007/s11814-017-0011-7

pISSN: 0256-1115
eISSN: 1975-7220

Effects of annealing temperature on Cu_2ZnSnS_4 (CZTS) films formed by electrospray technique

Liping Chen and Chinho Park†

School of Chemical Engineering, Yeungnam University, Gyeongsan 38541, Korea
(*Received 3 June 2016 • accepted 2 February 2017*)

Abstract−Cu_2ZnSnS_4 (CZTS) films were formed by an electrospray method, and the effects of annealing temperature on the properties of CZTS films were investigated. All CZTS films exhibited a kesterite structure with a preferred orientation of (112), (220) and (312), and did not show non-CZTS phases according to the annealing temperature. The grain size of CZTS films increased substantially in the temperature range of 300-450 °C, and the optical band-gap (E_g) of the films with increasing temperature decreased from 1.71 eV to 1.42 eV. Consequently, single-phased CZTS films were acquired without annealing process by electrospray method, and the annealing process improved the optical and structural properties of CZTS films. These results demonstrated that the CZTS films developed in this study has promising potential for the formation of high quality CZTS thin films in thin-film solar cells.

Keywords: Cu_2ZnSnS_4 (CZTS), Electrospray, Annealing, Temperature

INTRODUCTION

Many studies related to thin film solar cells have focused on the light-absorption layer materials, such as copper indium gallium selenide (CIGS), gallium telluride (CdTe) and silicon (Si) [1]. The solar cells applying these absorption materials exhibit conversion efficiencies beyond 20% [2]. On the other hand, these materials have some disadvantages in the context of electricity-production cost and/or environment-friendliness, such as the usage of rare-earth elements for CIGS, the toxicity of Cd in CdTe, and the high cost of Si solar cells. A large scaled area is required for most solar cells to acquire the desired electricity production; therefore, the cost and environmental considerations are essential prerequisites for the eco-economical production of electricity [3]. To solve these problems, it is necessary to develop earth-abundant and non-toxic absorber materials. Recently, more attention has been paid to the I_2-II-IV-VI_4 family, such as Cu_2ZnSnS_4 (CZTS) and $Cu_2ZnSnSe_4$ (CZTSe) [4]. These are not only earth-abundant and eco-friendly materials, but also have similar properties to CIGS [5]. Particularly, CZTS is a p-type semiconductor with a direct band gap of 1.4-1.5 eV having large absorption coefficient of 10^4 cm^{-1} [6], and the efficiency of CTZS solar cells has reached up to 12.6% recently [7].

The CZTS films are usually fabricated using vacuum-based depositions, including evaporation and sputtering methods [8-10]. However, these methods have low material utilization, relatively low throughput, difficulty for large-scale production, and high production cost [11]. On the other hand, non-vacuum methods, including solution-based deposition methods have some merits compared with vacuum-based methods, such as high throughput, large-scale process, facile fabrication process, and high material utilization [11,12]. However, non-vacuum methods were difficult to remove impurities in the CZTS films, and toxic materials were usually used to acquire the films [13-15]. Therefore, it's necessary to develop a non-toxic and eco-friendly solution-based process for the preparation of high quality CZTS films [16]. The electrospray method has been developed to deposit a range of thin films [17]. This method is possible for very fine droplets with a narrow distribution compared with various spray techniques [18]. The electrospray system is composed of a needle-type electrode, ground electrode and high voltage power, and the fine spray is formed easily by applying a high electric field between two electrodes [19]. This phenomenon arises due to the ionization of a precursor solvent and the repulsive force between identically charged particles under a high electric field, which prevents the aggregation of ionized particles [20]. In addition, preparations of precursors and deposition process are easy and inexpensive, because this technique is basically a non-vacuum deposition process. Therefore, the electrospray technique is considered as an effective method of forming CZTS thin films uniformly for economic production of CZTS thin film solar cells.

In this study, CZTS precursor thin films were formed on glass substrates using an electrospray method with $CuCl_2$, $ZnCl_2$, $SnCl_2$, and thiourea as precursor chemicals. The structural and optical properties of CZTS films were investigated, and the effects of annealing temperature on the films were studied in detail.

EXPERIMENTAL DETAILS

CZTS was synthesized using $CuCl_2$ (97%, Aldrich), $ZnCl_2$ (98%, Aldrich), $SnCl_2$ (98%, Aldrich), and thiourea (99%, Aldrich) as precursor materials with the 2 : 1 : 1 : 4 ratios of Cu, Zn, Sn, and S. Methanol (Aldrich) was used as low boiling point solvent (bp: 64.7 °C) and butyl carbitol (Aldrich) was used as high boiling point solvent (bp: 230-232 °C), respectively. First, $CuCl_2$ (2 mmol), $ZnCl_2$ (1 mmol) and $SnCl_2$ (1 mmol) were dissolved in methanol (5 ml),

†To whom correspondence should be addressed.
E-mail: chpark@ynu.ac.kr

and thiourea (8 mmol) was dissolved in a mixture of methanol (15 ml) and butyl carbitol (5 ml). An excess amount of thiourea was required to compensate for the loss of sulfur during pyrolysis. As-prepared solutions were mixed vigorously using an ultrasonic stirrer for 25 min at room temperature. Then as-prepared solution was put into a syringe with a volume of 5 ml, and the solution was introduced constantly into a needle with a flow rate of 0.6 mL/h using a syringe pump. The optimum flow rate was established to observe the spray shape by using a digital microscope (Digibird, Opt-500), and the shape began to be slightly unstable above 1 mL/h. The glass substrate was positioned onto a ground plate and the gap between the syringe needle and ground plate was kept at 4 cm. The substrate temperature was kept at 200 °C to remove the solvents of CZTS precursor during deposition process, and the applied voltage was set to 18 kV during the deposition. As-deposited CZTS films were annealed in a tube furnace at different temperatures (250, 350, 450, and 550 °C), and the growth rate of CZTS films was 2 μm/hr. Prior to the annealing process, the furnace was purged for 30 min using nitrogen gas and heated to the desired temperature. Then, the sulfur vapor was introduced into the furnace by using nitrogen carrier gas. The sulfur source was heated at 350 °C and the flow rate of nitrogen gas was 100 mL/min. The annealing process was carried out for 10 min under sulfur environment. After annealing, the samples were cooled to room temperature under nitrogen atmosphere.

The structural properties of the CZTS films were characterized by X-ray diffraction (XRD, Philips X'Pert-APD) using Cu-Kα radiation (0.1541 nm) with a current of 30 mA and a voltage of 40 kV, and a high-temperature XRD technique under Ar environment was performed to acquire the contour plot of XRD patterns as a function of annealing temperature (temperature range: 20 °C-580 °C, temperature step: 20 °C, heating time at each temperature step: 10 min). The vibrational properties of the films were studied by micro-Raman spectroscopy (Thermo Almega XR) with an excitation wavelength of 532 nm. The morphological images of the CZTS films were acquired by scanning electron microscopy (SEM, Hitachi S-4800), and the elemental ratio was analyzed by energy dispersive X-ray spectroscopy (EDAX). The optical properties of the films were examined by UV-Vis-NIR spectroscopy (Varian, Cary 5000).

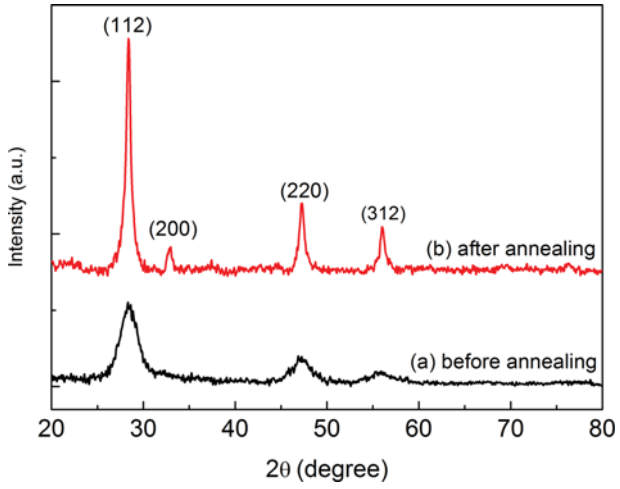

Fig. 1. XRD patterns of CZTS films at different annealing conditions; (a) as-deposited CZTS films using electrospray technique, and (b) annealed CZTS films at 550 °C for 10 min (film thickness: 2 μm).

RESULTS AND DISCUSSION

Fig. 1 presents the XRD patterns of as-deposited and annealed CZTS films, respectively. The XRD peaks centered at approximately 28°, 47° and 55° were mainly observed for both samples, and these peaks were attributed to the diffractions from (112), (220), and (312) planes, corresponding to the kesterite structure with a tetragonal unit cell (JCPDS No. 26-0575). The main differences in the XRD patterns for both samples were the full width at half maximum (FWHM) and the peak intensity; and the peak positions seldom changed upon annealing. To verify the dependency of the structural change of the CZTS films on the annealing temperature, XRD measurements of the as-deposited CZTS film were carried out at different temperatures. Fig. 2 shows the contour plot for the

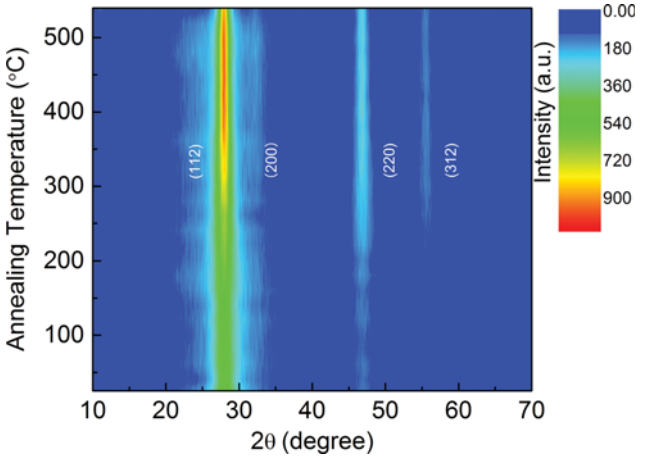

Fig. 2. Contour plot of the XRD patterns for CZTS films as a function of annealing temperature (film thickness: 2 μm, temperature step: 20 °C, heating time at each step: 10 min).

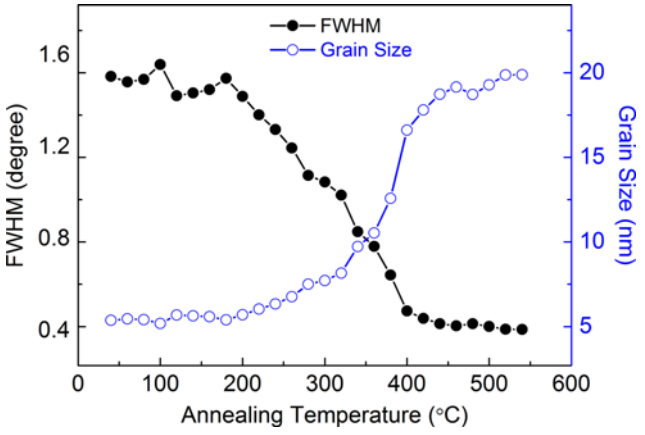

Fig. 3. FWHM of CZTS (112) peak and grain size of the CZTS films as a function of the annealing temperature.

XRD patterns of the CZTS films according to the annealing temperature change. The position of XRD peaks did not change as the annealing temperature changed, and there was no phase transition observed of the CZTS films. In addition, the FWHM of the XRD peaks decreased with increasing temperature, as shown in Fig. 3, which means that the grain size of the crystals in the films increased. The grain size was calculated using Scherrer's formula [21]:

$$D = \frac{k\lambda}{\beta\cos\theta} \quad (1)$$

where D is the crystalline size, k is a dimensionless shape factor with a value of 0.89, λ is the X-ray wavelength of 1.5418 Å, β is the full width at half maximum (FWHM), and θ is the Bragg angle. The grain size in the CZTS films exhibited an inverse relationship with respect to the tendency of the FWHM according to the annealing temperature, and increased significantly with increasing annealing temperature from 300 °C to 450 °C.

Fig. 4 shows the Raman spectra of CZTS films at different annealing temperatures. Normally, CZTS and ZnS exhibit similar XRD patterns [22], and Raman spectroscopy is very useful for distinguishing the difference between CZTS and ZnS phase. The strong peak centered at 336 cm^{-1} was attributed to the kesterite phase of CZTS, and the small peaks at 251 cm^{-1}, 285 cm^{-1} and 361 cm^{-1} were assigned to CZTS [22-24]. The Raman peaks for the ZnS phase, which were reported at 352 cm^{-1} and 271 cm^{-1}, were not observed directly in the Raman spectra [23]. Moreover, no other apparent secondary peaks were observed, confirming that all these samples were indeed CZTS. From these results, we concluded that all the CZTS films were formed during electrospray deposition process at 200 °C, and the annealing process only improved the crystallinity of the CZTS films. The formation of CZTS films at low temperatures could be explained by the following: the high voltage to the needle emitter led to the formation of small and highly charged liquid droplets, which dispersed rapidly due to the coulomb repulsive force, and were electro-sprayed on the substrates. Reactive metal ions, including Cu, Zn and Sn were re-combined on the glass substrates with S, and the chemical activity of the reactive metal ions could form CZTS films under low temperature conditions. In addition, the elemental ratio of Cu, Zn and Sn changed only slightly according to the annealing temperature, as shown in Table 1, and the Cu : Zn : Sn ratio was still around 2 : 1 : 1. So this is a strong evidence for the formation of stable CZTS films during film depositions.

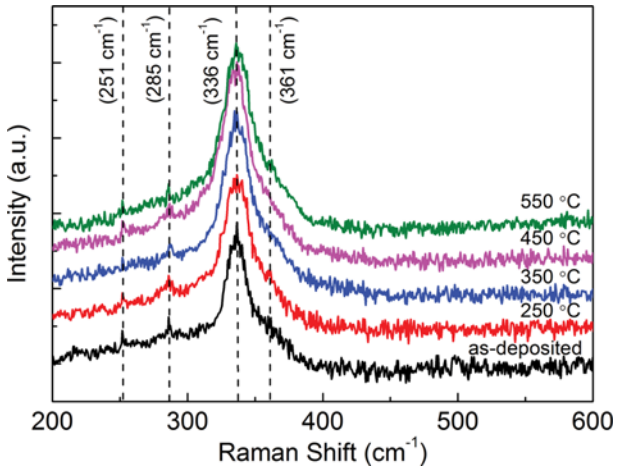

Fig. 4. Raman spectra of CZTS films obtained at different annealing temperatures (excitation wavelength of a laser source: 532 nm, film thickness: 2 μm).

Fig. 5 shows the cross-sectional SEM images of CZTS films

Table 1. Properties of CZTS films prepared at different annealing temperatures

Properties	Unit	Different annealing temperatures (°C)				
		As-deposited	250	350	450	550
Preferred orientation		(112) (220) (312)	(112) (220) (312)	(112) (220) (312)	(112) (220) (312)	(112) (220) (312)
FWHM	(degree)	1.447	1.236	0.802	0.428	0.406
Grain size	(nm)	5.60	6.55	10.10	18.92	19.97
Band-gap	(eV)	1.71	1.64	1.53	1.47	1.42
Absorption coefficient (@550 nm)	(10^4 cm^{-1})	1.69	1.73	1.84	2.16	2.48
Elemental ratio (Cu : Zn : Sn)		2 : 1.05 : 0.99	2 : 0.99 : 1.02	2 : 1.04 : 1.11	2 : 0.98 : 1.12	2 : 1.09 : 0.90

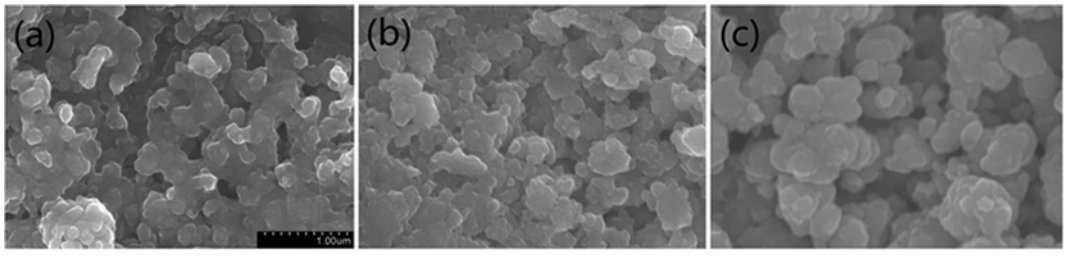

Fig. 5. SEM surface morphological images of CZTS films at different annealing temperatures: (a) as-deposited, (b) annealed at a temperature of 350 °C, and (c) 550 °C for 10 min under sulfur environment.

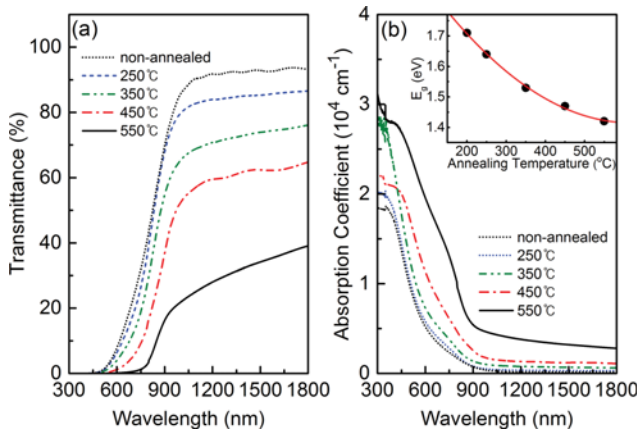

Fig. 6. Optical properties of the CZTS films (film thickness: 400 nm) according to the annealing temperatures: (a) Transmittance spectra and (b) absorption coefficient of CZTS films at different annealing temperatures (inset: optical band-gap of CZTS films as a function of annealing temperature).

annealed at different temperatures. In the as-deposited sample, small-sized CZTS particles were aggregated together; however, the size of the masses grew gradually with increasing annealing temperature. The size growth was attributed to a necking process between the adjacent masses and the tendency was consistent with the results of XRD patterns, as mentioned above.

Fig. 6(a) shows the transmittance spectra of CZTS films according to the different annealing temperatures. The transmittance of the CZTS films decreased and the absorption edge was red-shifted with the increase of the annealing temperature. The decrease in transmittance was directly related to the increase of absorption coefficient, as shown in Fig. 6(b). This result suggests that the change in structural properties, including grain size and crystallinity, played an important role in changing optical properties. Fig. 6(b) shows the optical energy band-gap (E_g) of the CZTS films according to the annealing temperature. E_g was calculated from the measured transmittance spectra data using Tauc's relation, which is given by the following [25]:

$$(\alpha h\nu)^2 = A(h\nu - E_g) \quad (2)$$

where α is the absorption coefficient, h is Planck's constant, ν is the frequency of the incident beam, and A is a constant. The E_g of the CZTS films decreased from 1.71 eV to 1.42 eV with increasing the annealing temperature to 550 °C. The change in E_g of the CZTS films according to the annealing temperature was closely related to the grain size, and the size was small enough to cause quantum confinement effects (QCE) [26]. The QCE usually occurs in nanoparticles (NPs) due to the size effect, and E_g in the semi-conductive NPs is blue-shifted with decreasing the size of NPs [27]. In this case, the grain size of the CZTS films increased from 5.6 nm to 20 nm with increasing the annealing temperature, and the value of E_g approached the bulk value of CZTS film (~1.4 eV) above an annealing temperature of 500 °C.

Consequently, the simple and inexpensive method developed in this study is suitable for a low temperature process that can produce high quality CZTS films. Table 1 lists the properties of the CZTS films deposited using the electrospray method according to the annealing temperature.

CONCLUSIONS

Cu_2ZnSnS_4 films were deposited on glass substrates using an electrospray method under low temperatures. To investigate the effects of temperature on the properties of CZTS films, the annealing temperature was changed from 250 °C to 550 °C. All the as-deposited CZTS films showed XRD peaks at (112), (220) and (312), indicating that the CZTS films have a kesterite structure, and there was no phase transition as the annealing temperature was increased. Moreover, the grain size of the CZTS films had a substantial growth when the annealing temperature was increased from 300 °C to 450 °C. All samples showed the characteristic Raman peaks for CZTS films at 251 cm^{-1}, 285 cm^{-1}, 336 cm^{-1}, and 361 cm^{-1}. Therefore, CZTS films were formed using electrospray method at 200 °C, and the annealing process only improves the crystallinity of the CZTS films. The optical band-gap of the CZTS films at different annealing temperatures decreased from 1.71 eV to 1.42 eV, and became closer to the optimal value required for an absorber material in solar cells. This change can be attributed to a decrease in grain size and the quantum confinement effects. These results confirm that the developed method is a non-toxic and inexpensive way to produce high quality CZTS films, and is suitable for low temperatures. The CZTS films deposited by the electrospray method are effective for photovoltaic devices and the films produced after annealing process can be with good crystallinity and optical properties.

ACKNOWLEDGEMENTS

This work was supported by the New & Renewable Energy Core Technology Program (No. 20143030011950) and the Human Resources Program in Energy Technology (No. 20154030200760) of the Korea Institute of Energy Technology Evaluation and Planning (KETEP) granted financial resource from the Ministry of Trade, Industry & Energy of Republic of Korea.

REFERENCES

1. Y. Wang, Y. Huang, A. Y. S. Lee, C. F. Wang and H. Gong, *J. Alloys Compd.*, **539**, 237 (2012).
2. H. T. Kim, D. Kim and C. Park, *Mol. Cryst. Liq. Cryst.*, **546**, 155 (2012).
3. S. Thiruvenkadam, D. Jovina and A. L. Rajesh, *Sol. Energy*, **106**, 166 (2014).
4. E. M. Mkawi1, K. Ibrahim1, M. K. M. Ali1 and A. S. Mohamed, *Int. J. Electrochem. Sci.*, **8**, 359 (2013).
5. V. Kheraj, K. K. Patel, S. J. Patel and D. V. Shah, *J. Cryst. Growth*, **362**, 174 (2013).
6. S. M. Pawar, B. S. Pawar, A. V. Moholkar, D. S. Choi, J. H. Yun and J. H. Moon, *Electrochim. Acta*, **55**, 4057 (2010).
7. R. R. King, A. Boca, W. Hong, X.-Q. Liu, D. Bhusari, D. Larrabee, K. M. Edmondson, D. C. Law, C. M. Fetzer, S. Mesropian and N. H. Karam, *European Photovoltaic Sol. Energy Conference and Exhibi-*

tion, **24**, 21 (2009).
8. K. Wang, O. Gunawan, T. Todorov, B. Shin, S. J. Chey, N. A. Bojarczuk, D. Mitzi and S. Guha, *Appl. Phys. Lett.*, **97**, 143508 (2010).
9. C. P. P. Bjorkman, J. Scragg, H. Flammerrsberger, T. Kubart and M. Endoff, *Sol. Energy Mater. Sol. Cells*, **98**, 110 (2012).
10. N. Kamoun, H. Bouzouita and B. Rezig, *Thin Solid Films*, **515**, 5949 (2007).
11. K. Tanaka, N. Moritake, M. Oonuki and H. Uchiki, *Jpn. J. Appl. Phys.*, **47**, 598 (2008).
12. B. L. Guo, Y. H. Chen, X. J. Liu, W. C. Liu and A. D. Li, *AIP Advances*, **4**, 097115 (2014).
13. K. Woo, Y. Kim and J. Moon, *Energy Environ. Sci.*, **5**, 5340 (2012).
14. M. L. Jiang, F. Lan, X. Z. Yan and G. Y. Li, *Phys. Status Solidi RRL*, **8**, 3 (2014).
15. H. X. Wang, *International J. Photoenergy*, **10**, 801292 (2011).
16. K. Kim, I. Kim, Y. Oh, D. Lee, K. Woo, S. Jeong and J. Moon, *The Royal Soc. Chem.*, **16**, 4323 (2014).
17. D. Song, W. Kim, K. Mahmood, H. W. Kang, S. B. Park, S. Park and J. Han, *J. Alloys Compd.*, **567**, 89 (2013).
18. A. Jaworek, *J. Mater. Sci.*, **42**, 266 (2007).
19. G. J. V. Berkel, S. A. McLuckey and G. L. Glish, *Anal. Chem.*, **64**, 1586 (1992).
20. S. J. Gaskell, *J. Mass Spectrom.*, **32**, 677 (1997).
21. N. M. Shinde, R. J. Deokate and C. D. Lokhande, *J. Anal. Appl. Pyrolysis*, **100**, 12 (2013).
22. A. Emrani, P. Vasekar and C. R. Westgate, *Sol. Energy*, **98**, 335 (2013).
23. S. Huang, W. J. Luo and Z. G. Zou, *J. Phys. D: Appl. Phys.*, **46**, 235108 (2013).
24. P. A. Fernandes, P. M. P. Salomé and A. F. da Cunha, *J. Alloys. Compd.*, **509**, 7600 (2011).
25. H. S. Yoo, J. H. Kim and L. X. Zhang, *Curr. Appl. Phys.*, **12**, 1052 (2011).
26. A. Khare, A. Wliis, L. M. Ammerman, D. J. Norris and E. S. Aydil, *Chem. Compd.*, **47**, 11721 (2011).
27. C. D. Kim, H. T. Kim, B. K. Min and C. Park, *Mol. Cryst. Liq. Cryst.*, **602**, 151 (2014).